JACS
JOURNAL OF THE AMERICAN CHEMICAL SOCIETY
Article
pubs.acs.org/JACS

Development of Cell-Active N^6-Methyladenosine RNA Demethylase FTO Inhibitor

Baoen Chen,[†,⊥] Fei Ye,[†,⊥] Lu Yu,[‡,⊥] Guifang Jia,[§] Xiaotian Huang,[†] Xueju Zhang,[†] Shuying Peng,[†] Kai Chen,[∥] Meining Wang,[†] Shouze Gong,[†] Ruihan Zhang,[†] Jinya Yin,[†] Haiyan Li,[†] Yiming Yang,[†] Hong Liu,[†] Jiwen Zhang,[†] Haiyan Zhang,[†] Ao Zhang,[†] Hualiang Jiang,[†] Cheng Luo,*[,†] and Cai-Guang Yang*[,†,¶]

[†]State Key Laboratory of Drug Research, Shanghai Institute of Materia Medica, Chinese Academy of Sciences, Shanghai 201203, China

[‡]Shenyang Pharmaceutical University, Shenyang 110016, China

[§]College of Chemistry and Molecular Engineering, Peking University, Beijing 100871, China

[∥]Department of Chemistry, University of Chicago, Chicago, Illinois 60637, United States

[¶]State Key Laboratory of Applied Organic Chemistry, Lanzhou University, Lanzhou 730000, China

Supporting Information

ABSTRACT: The direct nucleic acid repair dioxygenase FTO is an enzyme that demethylates N^6-methyladenosine (m^6A) residues in mRNA *in vitro* and inside cells. FTO is the first RNA demethylase discovered that also serves a major regulatory function in mammals. Together with structure-based virtual screening and biochemical analyses, we report the first identification of several small-molecule inhibitors of human FTO demethylase. The most potent compound, the natural product rhein, which is neither a structural mimic of 2-oxoglutarate nor a chelator of metal ion, competitively binds to the FTO active site *in vitro*. Rhein also exhibits good inhibitory activity on m^6A demethylation inside cells. These studies shed light on the development of powerful probes and new therapies for use in RNA biology and drug discovery.

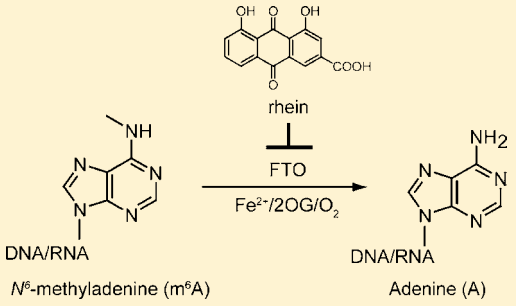

INTRODUCTION

The fat mass and obesity-associated FTO gene is the first and most robust obesity-risk gene discovered in genome-wide association studies.[1−4] FTO protein has been demonstrated to influence human obesity and energy utilization in up to half the world's population.[5,6] In addition, FTO is reported to be involved in various disease processes, including cardiovascular diseases,[7,8] type II diabetes,[9] Alzheimer's disease,[10] and breast cancer.[11] Such discoveries make FTO an increasingly interesting target with respect to its functional links to human diseases. Particularly, FTO enzyme is the first RNA demethylase discovered that also serves a major regulatory function in mammals.[12] Thus, small molecules inhibiting FTO are not only important to possibly provide unique opportunities for treating diseases such as obesity and cancer, but may also have a profound impact on the study of fundamental RNA demethylation biology. Unlike siRNA that removes the entire protein, the small-molecule inhibitor only shuts down the activity of FTO target. Present and future studies that focus on the impact of the activity of FTO will likely lead to new insights at the forefront of RNA epigenetics in chemical biology and drug discovery.[13]

FTO belongs to the family of Fe^{2+}- and 2-oxoglutarate (2OG)-dependent AlkB dioxygenases that also includes human homologues ALKBH1−8.[14,15] ALKBH1 and ALKBH3 have been shown to catalyze the oxidative demodification of methylated bases in single-stranded RNA (ssRNA).[16,17] A related enzyme, ALKBH8, catalyzes the hydroxylation of a wobble uridine in a specifically hypermodified tRNA.[18,19] Similarly, FTO can oxidatively demethylate N^3-methyluridine (m^3U) in ssRNA *in vitro*,[14,20] but it has relatively lower repair activities compared to other AlkB family proteins.[21] Remarkably, N^6-methyladenosine (m^6A), which was first discovered in mRNA decades ago,[22] has recently been identified as an endogenous substrate of FTO in mammalian cells.[12] The elucidation of dynamic regulation of mRNA post-transcriptional modifications is just beginning; thus, the physiological function of the ubiquitous m^6A post-transcriptional modification remains largely unclear. The fact that the function of the obesity-risk factor FTO is to demethylate m^6A in mRNA clearly indicates a novel and reversible regulatory mechanism that presents in mammalian cells and stimulates further efforts to

Received: July 2, 2012
Published: October 9, 2012

dx.doi.org/10.1021/ja3064149 | J. Am. Chem. Soc. 2012, 134, 17963−17971

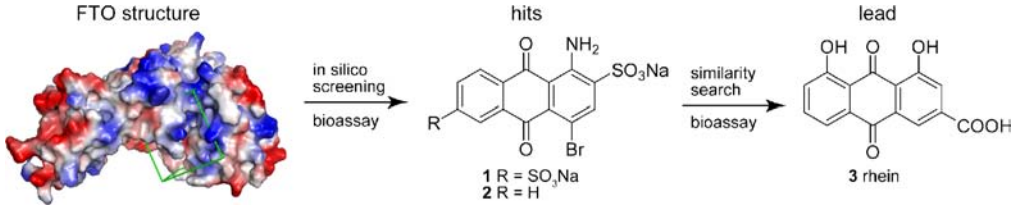

Figure 1. Virtual screening for binding of compounds at the FTO active site. Shown is an illustration of the virtual screening procedure using the crystal structure of FTO (PDB code 3LFM)[26] as a docking target. Chemical structures of hits **1** and **2** and lead compound **3** are also given.

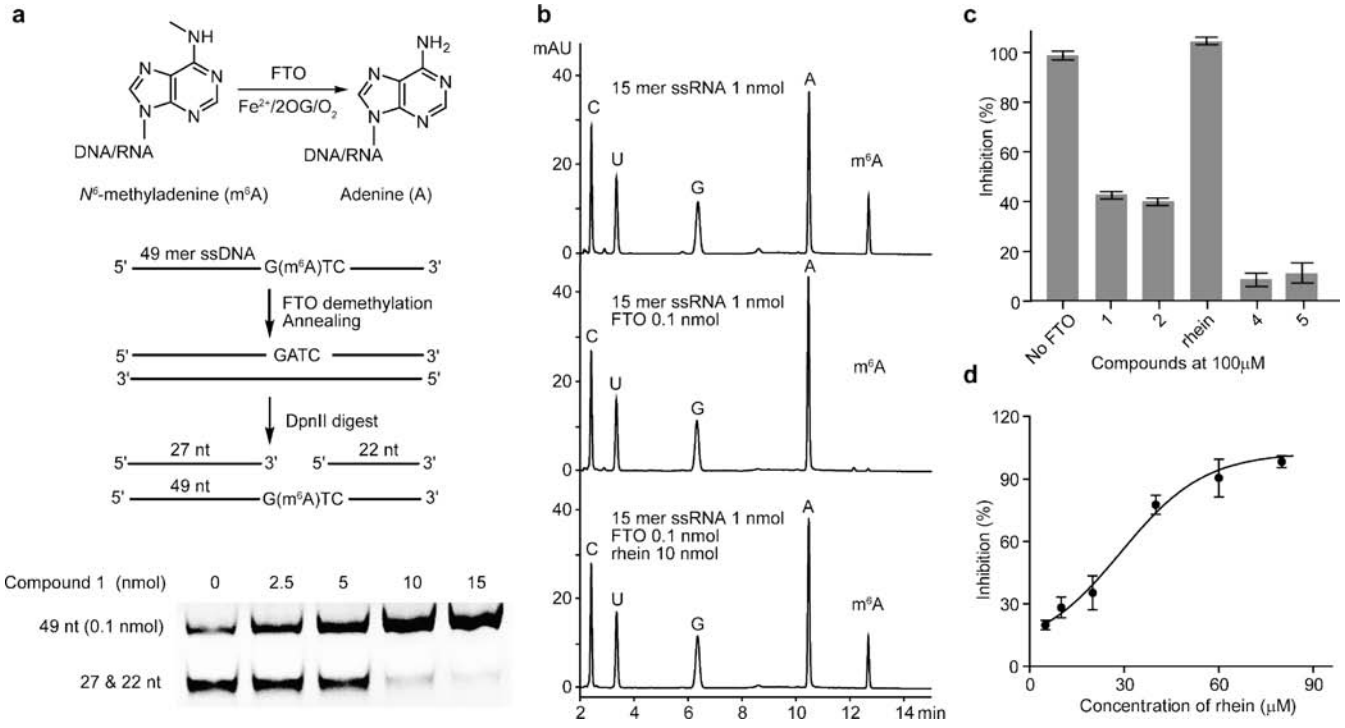

Figure 2. Inhibition of FTO demethylation of ssDNA and ssRNA substrates. (a) Inhibition of FTO demethylation of m^{6}A in ssDNA. The *Dpn*II digestion assay is shown in the top panel. The bottom panel is PAGE analyses showing FTO repair of m^{6}A in ssDNA in the presence of compound **1**. The upper band is 49-mer dsDNA, which contains m^{6}A, and the lower bands show the mixtures of 22- and 27-mer dsDNA products of *Dpn*II digestion. (b) Inhibition of FTO demethylation of m^{6}A in ssRNA. Shown is HPLC trace of repair of m^{6}A in ssRNA (1 nmol) by FTO (0.1 nmol) with rhein (10 nmol). (c) Bar presentation of FTO inhibitory rates by different compounds. Reactions are carried out in the same scale as in (b) with different compounds (10 nmol). The relative inhibitory percentage is estimated on the area under the m^{6}A peak in the HPLC trace. (d) Representative FTO inhibitor rhein dose–response assay. The inhibitions of FTO demethylation m^{6}A in ssRNA are assayed in triplicate with varying concentrations of rhein, and the inhibitory activities are quantified in the HPLC trace. Standard deviation is indicated.

explore m^{6}A modifications and related enzymes. Recently, it has been demonstrated that RNA decorated with m^{6}A is widespread in a large fraction of cellular mRNA and plays a fundamental regulatory role in gene expression.[23] In addition, FTO has been shown to demethylate diverse mRNAs, which reveals that the regulation of m^{6}A by FTO likely influences a variety of biological pathways relevant to cellular signaling and disease.[24] All this evidence suggests that FTO has an essential role in the control of other gene expression and protein translation processes involved in the regulation of diseases such as obesity and cancer.[25] These discoveries have opened up novel therapeutic possibilities, including targeting mRNA demethylases with small molecules.

The recently reported crystal structure of FTO has offered insights into cofactors and substrate binding sites.[26] Taken together with the extensive structural and mechanistic studies of AlkB family proteins,[27−31] these studies enable the rational design and development of inhibitors targeting RNA demethylases. To our knowledge, no inhibitor has been developed for human nucleic acid demethylases, in particular mRNA demethylase FTO.[32,33] Here, we report our initial steps toward a structure-based *in silico* high-throughput screening and further structural optimization, thus leading to the identification of the natural product rhein as the first potent FTO inhibitor. Unlike most of the reported 2OG-type inhibitors that are either chemical mimics of 2OG or chelators of iron,[32] the ability of rhein to inhibit FTO is novel. We use a combination of biochemical and biophysical approaches to investigate this unique mechanism of FTO inhibition through rhein and reveal that this compound inhibits FTO by competitively binding the catalytic domain against ssRNA substrate. We also show that rhein alters m^{6}A levels in mRNA inside cells. Together, the identification of rhein as the first competitive inhibitor of FTO demethylase paves the way for the development of selective and specific inhibitors and functional probes to target mRNA demethylases on the cellular level for both biological and therapeutic purposes.

dx.doi.org/10.1021/ja3064149 | J. Am. Chem. Soc. 2012, 134, 17963−17971

Scheme 1. Three Groups of FTO Inhibitors

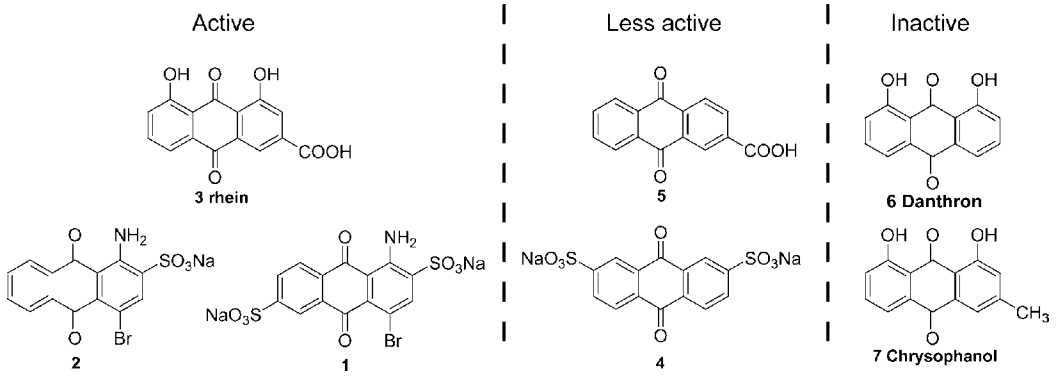

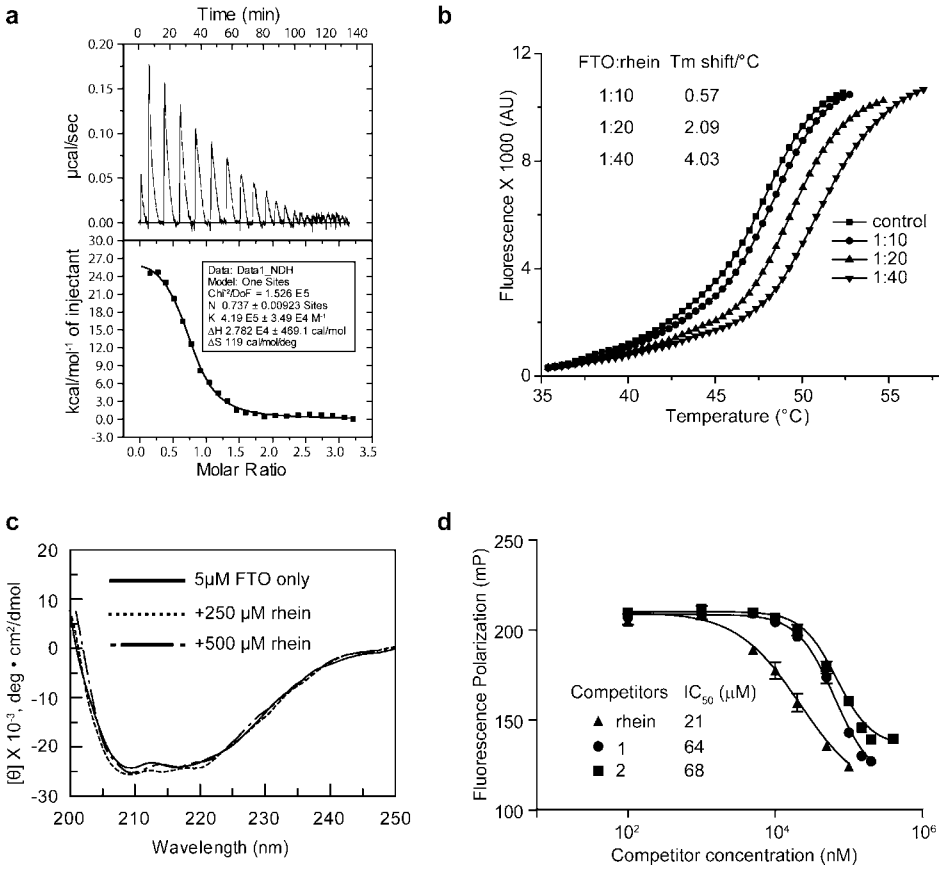

Figure 3. Binding studies of FTO and inhibitors. (a) ITC binding curve for FTO and rhein. This experiment yields a K_d value of 2.4 μM. (b) Thermal shift assay to test the stabilization of FTO by rhein. Shown are graphs of unfolding transition of 1.25 μM FTO in the presence of 12.5, 25, and 50 μM rhein, respectively. (c) CD spectra of FTO in the presence of rhein at 250 and 500 μM, respectively. (d) Displacement of ssDNA from FTO by three inhibitors. Determination of the inhibitory ability of compounds **1**, **2**, and rhein was found through a competitive fluorescence polarization assay. The IC_{50} values of inhibitors under the conditions of this experiment are in the range of 21−68 μM.

RESULTS AND DISCUSSION

Virtual Screening. The crystal structure of FTO in complex with m^3T (PDB code 3LFM) was used as a docking target (Figures 1 and S1).[26] Residues within 6 Å around m^3T were defined as binding sites. The drug-like SPECS database, which contains about 100 000 compounds, was selected for subsequent docking studies. After virtual screening, 114 compounds were selected for experimental validation, and compounds **1** and **2** were found to be active for FTO inhibition. We used this core structure as a hit to perform a similarity search through an in-house database of known drug therapies to obtain the compound rhein (**3**).

Inhibition of FTO Demethylation *in Vitro*. To validate the inhibitors identified in the virtual screening, we performed several biochemical assays to measure the inhibition of FTO demethylation on different single-stranded nucleic acids containing m^6A in the sequence. The previously published restriction endonuclease digestion assay was first adopted to evaluate the inhibition of FTO demethylation on m^6A in ssDNA by compound **1**.[29] The reactions were run with 0.1 nmol of FTO, 0.1 nmol of 49-mer ssDNA, and varying concentrations of compound **1** at room temperature for 2 h. As

dx.doi.org/10.1021/ja3064149 | J. Am. Chem. Soc. 2012, 134, 17963−17971

shown in Figure 2a, we observed good repair activity of FTO demethylation in the control reaction, indicating that the FTO enzyme was in the active form. FTO repair activity was inhibited by compound **1** in a concentration-dependent manner. The demethylation activity of FTO was completely abolished when 10-fold excess of compound **1** was presented in the reaction system with respect to ssDNA substrate (Figure 2a).

To confirm the observed inhibition of FTO demethylation on ssDNA by compound **1**, a different HPLC-based detection assay was carried out using ssRNA substrate.[34] As shown in Figure 2b, nucleosides C, U, G, A, and m^6A could be clearly separated (top panel) in HPLC trace, while the corresponding m^6A absorbent peak disappeared in the presence of 0.1 equiv of FTO (middle panel). This result indicated an FTO-mediated conversion of m^6A to normal A under the standard repair condition. After treatment with 10 equiv of rhein to ssRNA under the same reaction conditions, FTO repair activity was completely abolished, as evidenced by the remaining m^6A peak (bottom panel in Figure 2b). Other compounds obtained from the *in silico* screening showed weak inhibition of FTO demethylation on ssRNA compared to rhein under the same conditions (Figures 2c and S2a). Similar to compound **1** inhibition on ssDNA substrate, rhein inhibition of m^6A demethylation on ssRNA was also observed to occur in a concentration-dependent fashion (Figure S2b). We have determined the dose-dependent response of rhein inhibition of FTO demethylation on an m^6A-containing 15-mer ssRNA at pH 7.5 and 25 °C. The IC_{50} value was measured to be around 30 μM using the HPLC assay (Figures 2d and S2b).

SAR Analyses. The active compounds represent a class of flavonoid natural products, which bear functional substitutions of acidic groups and several hydrogen bond donor/acceptor motifs. To obtain structure−activity information to help understand the interaction mode between the FTO protein and inhibitors, we tested additional commercially available compounds containing the core structure of both compound **1** and rhein (Scheme 1). First, the hydroxyl/amino groups on the core of the three-ring system significantly contributed to the inhibition of FTO demethylation. The structurally related analogues of rhein (the most potent FTO inhibitor yet identified), compound **4** and **5** both showed very weak inhibitory activities on FTO repair (Figures 2c and S2a). Furthermore, we observed that acidic groups, either sulfonate or carboxylate at the 2- or 3-position of the phenyl ring, are required for inhibition. This can be understood from the observation that Danthron (**6**) or Chrysophanol (**7**) did not inhibit FTO demethylation of nucleic acid where a hydrogen or methyl group substituted the carboxylic groups of rhein. Lastly, diacidic groups seem to be unnecessary for maintaining potent inhibition activity. Compound **2** bearing one sulfate group displayed inhibition activity comparable to that of compound **1**, which contains two sulfate substitutions within the core structure (Figure 2c). This preliminary SAR data demonstrates that both the acidic and hydroxyl/amino functional groups are important for potent inhibitory activity against FTO demethylase *in vitro*, thus implicating these functional groups in protein binding.

FTO Small-Molecule Binding Studies. In order to more precisely validate these potential FTO inhibitors, we utilized multiple methods to measure direct interactions between FTO and small-molecule compounds. We used isothermal titration calorimetry (ITC) to determine that the equilibrium dissociation constant (K_d) between rhein and FTO is around 2.4 μM (Figure 3a). The binding interaction is entropy driven (ΔH = 27.8 kcal mol^{-1}, ΔS = 119 cal mol^{-1} K^{-1}). The inhibitors also demonstrated binding activities to purified FTO protein in surface plasmon resonance (SPR) assays, yielding K_d = 8.3, 11.5, and 18.2 μM for compounds **1**, **2**, and rhein, respectively (Figure S3). A third independent measurement, a fluorescence-based thermal shift assay, was also employed to further test the interaction of rhein and FTO protein. As shown in Figure 3b, the presence of rhein shifted the native FTO protein melting temperature (T_m) more than 4 °C higher when 40-fold excess of rhein was added to FTO solution. It has been suggested that flavonoid natural products act as nonspecific inhibitors of 2OG dioxygenases and are likely inhibited by affects on protein structure/aggregation.[32] To test whether rhein caused a conformation change of FTO enzyme, we performed a circular dichroism (CD) experiment. When rhein was added to a concentration of 500 μM, 100-fold excess over FTO, we observed subtle changes in the CD spectra, indicating there were no gross structural perturbations of the FTO protein (Figure 3c).

Next, a rigorous experiment using fluorescence polarization (FP) assay was carried out to test the ability of displacement of nucleic acid binding to FTO by small-molecule inhibitors. As shown in the FP assay (Figure 3d), analyses of the competition-binding curves yield IC_{50} values for competitors **1**, **2**, and rhein of 64, 68, and 21 μM, respectively, thus demonstrating that rhein is the most potent inhibitor against FTO binding to ssDNA. The acidic analogues of rhein, compounds **4** and **5**, were detected to have much weaker IC_{50} values of >350 and >250 μM compared to rhein in the FP assay (Figure S4a). These data are consistent with the relatively weak inhibitory activities observed so far of these two compounds in the HPLC assay (Figure 2c). Compounds **6** and **7**, two derivatives of rhein, failed to decrease the fluorescence polarization signals under the same conditions (Figure S4b), suggesting that the lack of the acidic functional groups on the core structure prevents small molecules from binding to FTO protein. This result partially explains the previous observation that neither compound **6** nor **7** showed any detectable inhibition of FTO demethylation, even at high concentration (Scheme 1). In addition, the generic inhibitor of AlkB protein, compound **8** (Figure S4c), exhibited weak inhibition of FTO repair of m^6A in ssRNA (Figure S4d).[35] However, FP assay showed that this compound failed to disrupt FTO/ssDNA binding (Figure S4b). This result reveals the role of compound **8** as either a chelator of iron in solution or an occupier of the cofactor 2OG binding site, rather than partially taking over the m^6A-binding pocket to prevent flipping into the active site. Notably, the recently solved complex structure of AlkB/compound **8** clearly shows how the small molecule binds to the FTO active pocket.[35] Although the conformation of active sites may vary among different nucleic acid demethylases, AlkB and FTO for example, we still could speculate that compound **8** might bind to the FTO active site in a mode similar to that observed in AlkB, which could not disrupt nucleotide binding. Together, these biophysical binding measurements confirmed that the inhibitors, which we have identified, competitively bind to the nucleic acid demethylase FTO.

Kinetic Study of Inhibition Mode. We performed a detailed mechanistic study to clarify the mode of rhein inhibition to FTO enzyme. To rule out the possibility of inhibition by simple metal ion chelation, we tested FTO

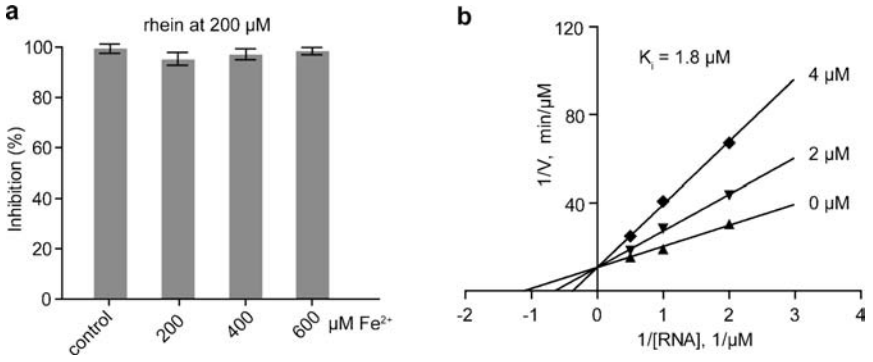

Figure 4. Studies of FTO inhibition modes. (a) Inhibitory ratios of FTO demethylation on ssRNA with excess Fe^{2+} at varying concentrations. All reactions were performed at room temperature in triplicate, and the error bars are shown. (b) Study of FTO-inhibition kinetics by rhein. Initial rates of FTO-catalyzed demethylation of m^6A were determined at ssRNA concentrations ranging from 0.5 to 2.0 μM in the presence of rhein at 0, 2, and 4 μM, respectively.

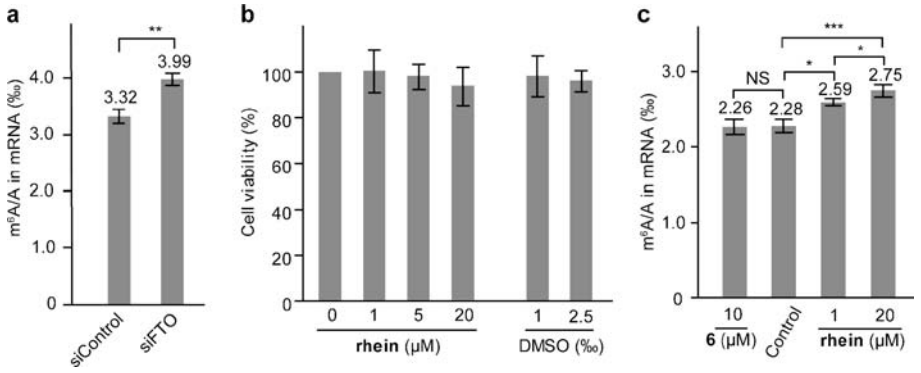

Figure 5. Cellular activity of rhein. Student's *t* test reveals significance: *, $P < 0.05$; **, $P < 0.01$; ***, $P < 0.001$. Error bars are means ± s.e.m. ($n = 3$ or 4). (a) Increase of m^6A content in mRNA of siRNA treated BE(2)-C cells. Quantification of the m^6A/A ratio in mRNA was determined by LC-MS/MS. (b) Measurement of BE(2)-C cells' viability in the presence of inhibitor using MTT assay. Data were obtained from four independent tests. (c) Inhibition of m^6A demethylation in mRNA by rhein in BE(2)-C cells.

demethylation of ssDNA and ssRNA with compound **1** and rhein, respectively, under various concentrations of Fe^{2+}. We found that the activity of FTO demethylation of m^6A in single-stranded nucleic acids in the presence of inhibitor rhein or compound **1** could not be restored up to a 3-fold molar excess of Fe^{2+} with respect to the inhibitor (Figures 4a and S5a,b). Together with the measured binding between inhibitors and FTO, these results suggest that small-molecule inhibitors shut down FTO activity not by chelating Fe^{2+} ion in solution, but rather by competitively binding to FTO enzyme in order to hinder m^6A repair. In contrast, the natural product quercetin (**9**) (Figure S5c), a known inhibitor for *E. coli* AlkB, was also analyzed for the inhibition of FTO demethylation.[36] As speculated, this compound was observed to inhibit FTO demethylation of m^6A residue in ssRNA; however, its inhibition is Fe^{2+} dependent. The demethylation activity of FTO could be partially recovered when the excess Fe^{2+} exists in the repair system (Figure S5d). This result reveals the mechanism by which quercetin chelates metal ions to inhibit the process of FTO demethylation.

To distinguish between competitive, noncompetitive, and uncompetitive modes of inhibition, we determined detailed reaction kinetics of rhein inhibition on FTO demethylation. The kinetics studies were performed at 25 °C and pH 7.5 using a 15-mer m^6A-containing ssRNA substrate. In the absence of the inhibitor rhein, the K_m value of FTO enzyme was determined to be 0.86 μM, which is comparable to previously reported data (Figure S6a).[12] The inhibitor rhein was observed to cause an increase in K_m to 1.93 and 2.94 μM under concentrations of 2 and 4 μM, respectively (Figure S6b,c), with no changes in V_{max} (Figure 4b). The Lineweaver–Burk analyses revealed that the K_i for rhein was 1.8 μM, which is comparable to the observed K_d value (2.4 μM) of FTO protein and ssDNA substrate measured in the ITC experiment. These data reveal that rhein acts as a competitive inhibitor of FTO protein with respect to the nucleic acid substrate. Given the potential for a redox mechanism of rhein in activation, it should be noted that rhein was experimentally demonstrated to be a reversible inhibitor on FTO demethylation (Figure S6d).

Off-Target Selectivity Analyses. Rhein is one of the major bioactive components in rhubarb (Dahuang), a famed and traditional Chinese medicine derived from the rhizome of *Rheum palmatum* and relative species, and which shows a diverse variety of bioactivities in different pathways;[37−39] however, its cellular targets remain largely unknown.[40] To evaluate the enzyme selectivity of rhein, we first examined its activity against several other AlkB human isoforms *in vitro*, for example, the house-keeping ALKBH2 that specifically demethylates the cellular N^1-methyladenosine (m^1A) modification. We found that rhein biochemically inhibited ALKBH2 activity with IC_{50} value on the same order of magnitude as seen for FTO (data not shown). Next, we checked the NIH Molecular Libraries Probe Development Center Network (MLPCN) program. Rhein has been subject to a number of bioactivity or

dx.doi.org/10.1021/ja3064149 | J. Am. Chem. Soc. 2012, 134, 17963−17971

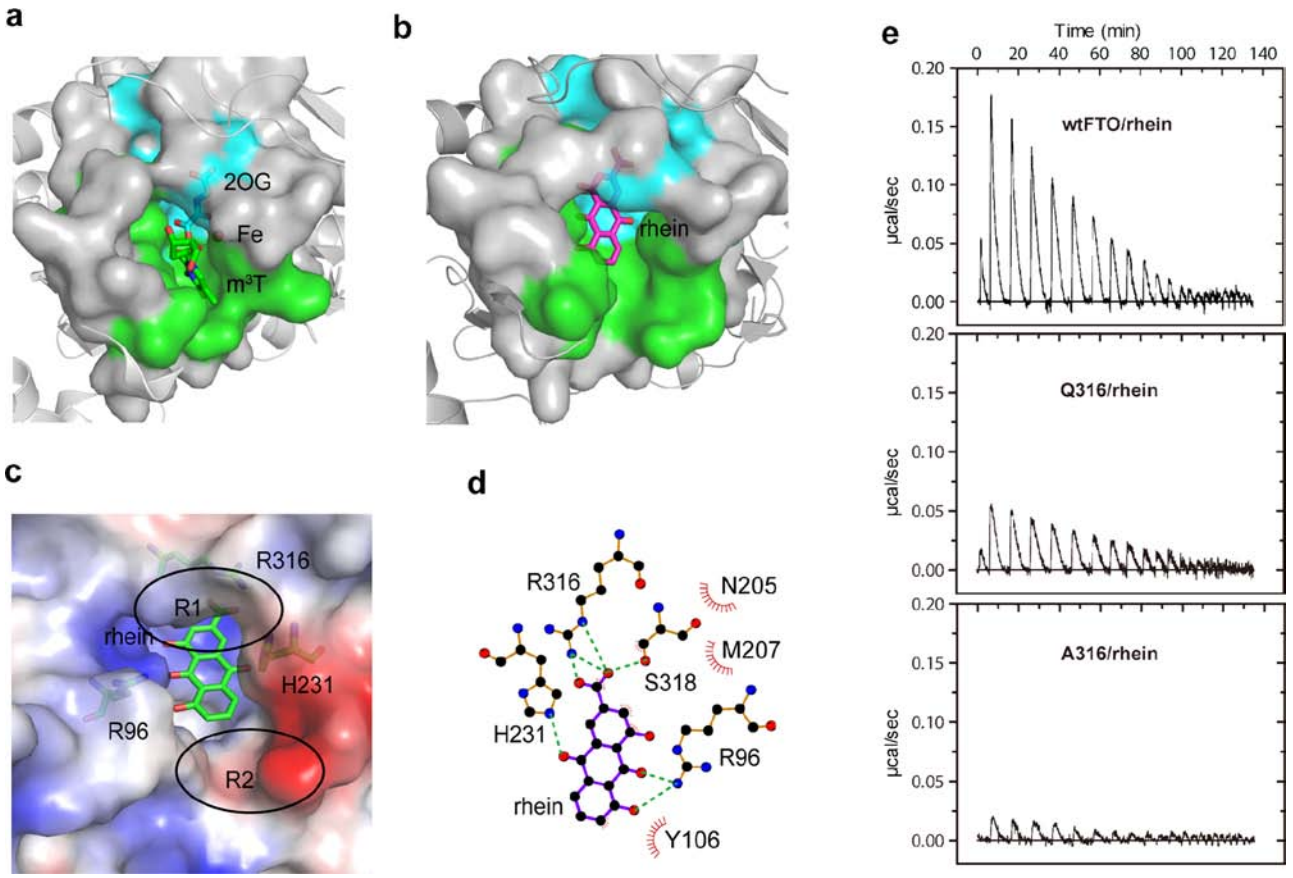

Figure 6. Molecular model of rhein/FTO complex. (a) Surface representative cofactors and substrate binding at active pocket in FTO crystal structure (PDB code 3LFM). The 2OG and oxygen-binding region is colored in cyan, and the m^3T site in green. (b) Molecular modeling of rhein/FTO complex. The binding pocket is shown in the same orientation as in (a). (c) A close view of the interactions between rhein and FTO in the active pocket. The environmental residues involved in the rhein interaction are shown. (d) Schematic diagram showing putative interactions between FTO and rhein. Residues involved in the hydrophobic interactions are shown as starbursts, and hydrogen-bonding interactions are denoted by dotted green lines. (e) ITC assays of rhein interacting with the wild-type protein and two FTO mutants.

inhibitor discovery high-throughput screenings via this program.[41] Rhein was reportedly active in about 58 over 829 (7%) cell-based and biochemical screens. Among these screenings, rhein was observed to inhibit the human Jumonji domain containing 2A and 2E (JMJD2) histone demethylases, which are also Fe^{2+}- and 2OG-dependent hydroxylases; for more distantly related 2OG-dependent hydroxylases such as prolyl-4-hydroxylase, however, rhein did not show inhibition activity in the *in vitro* screenings. Additionally, rhein was not active to inhibit HDAC3 histone deacetylase or APOBEC3 DNA deaminases, which belong to transition metal-dependent histone or nucleic acid modifying enzymes.

Cell-Based Activity. Under physiological conditions, m^6A has so far been identified as the best substrate for FTO *in vivo*.[12] We explored whether rhein would modulate m^6A modifying levels in mRNA inside cells. BE(2)-C is a clone of the SK-N-BE(2) neuroblastoma cell line. BE(2)-C cells were transiently transfected with FTO siRNA (Supporting Information) for 48 h.[12] The total mRNA was isolated by poly(dT) oligo magnetic beads followed by the depletion of rRNA and digested into nucleosides (Figure S7), and the cellular concentration of m^6A levels was determined by LC-MS/MS. The total contents of m^6A and A were quantified on the basis of a standard curve obtained by using pure standards, from which the m^6A/A ratio was calculated (Figure S8). Notably, the detected cellular ratio of m^6A/A ranges between 2.0 and 4.0‰, which is consistent with the reported abundance: about 1 m^6A per 2000 nucleotides in transcriptome.[23] We found that siRNA knockdown of FTO increased m^6A content in mRNA in BE(2)-C cells (Figure 5a), revealing that FTO also regulated m^6A modification in BE(2)-C cells in an FTO activity-dependent manner as seen for other cell lines, such as HeLa and 293FT.[12] After BE(2)-C cells were treated with inhibitor rhein at a concentration of 20 μM for 24 h, the cells were still healthy (Figures 5b and S9a), and the total mRNA isolated from cells showed a notable increase of the modifying m^6A level with significance of a *P*-value of less than 0.001 compared to untreated cells (Figure 5c). The ability of rhein to inhibit m^6A demethylation in mRNA displays a phenotype in a concentration-dependent manner. In a negative control experiment, compound **6**, the structural analogue of rhein, which was biochemically inactive on FTO inhibition *in vitro* (Scheme 1), did not show inhibition of the demethylation of cellular m^6A at 10 μM (Figures 5c and S9b). We tend to conclude that the increase of the m^6A distributions was caused by the presence of rhein inside cells; in addition, this is likely the result of the direct inhibition of cellular demethylation via FTO and perhaps other members of nucleic acid demethylases by rhein. Further characterization of the cellular specificity of rhein is also important to prove its use as a cellular probe for nucleic acid demethylases in the future research.

dx.doi.org/10.1021/ja3064149 | J. Am. Chem. Soc. 2012, 134, 17963−17971

Molecular Modeling. The biophysical analyses combined with the kinetics study suggest that rhein competitively binds to the active site of FTO in order to hinder nucleic base binding. No structures of flavonoid-type inhibitors in complex with 2OG dioxygenases have ever been reported. Therefore, a structural model would incite considerable interest. Molecular modeling was performed in order to understand the molecular detail for the binding mode of rhein at the FTO active site (Supporting Information). This modeling revealed that rhein occupies the binding sites of m^3T, 2OG, and Fe^{2+} in order to disrupt cofactor and substrates binding (Figures 6a,b and S10, and Table S1). The negative-charged carboxyl of rhein was positioned to interact with the extensive positively charged region near residue R316 (R1 region in Figure 6c), while pointing away from region R2 where the environment was negatively charged as a result of the presence of D233. In addition to extensive salt bridge interactions, R316 also made several hydrogen-bonding contacts with rhein (Figure 6d), thus suggesting a key role of R316 in mediating an interaction between rhein and FTO. The decomposed binding energy validates that these electrostatic interactions between R316 and rhein significantly contribute to the binding of rhein (Table S2). R316 has been identified as a crucial motif involved in 2OG binding at the active site because the FTO mutant of R316 completely lost repair activity.[12] To validate the hypothesis of the important role of R316 in the modeling study, we performed the ITC binding experiment with rhein and FTO mutants, Q316 and A316, respectively. As shown in Figure 6e, mutation of R316 to Q316 significantly weakened the binding; particularly, the A316 mutant almost completely abolished the interaction between rhein and protein. This molecular modeling study combined with biophysical/biochemical evidence revealed that the inhibition of FTO by rhein most likely occurs through directly binding against nucleic acids or in a manner of competition with the 2OG cofactor at the active site, or both, rather than by chelating free iron in solution. Currently, we still cannot rule out the possibility of multiple orientations of rhein binding to FTO (Figure S10); therefore, the crystal structure of small molecules in complex with FTO has yet to be determined. Such a structure would provide the detailed interaction mode of the active site.

CONCLUSIONS

In conclusion, although several inhibitors toward 2OG dioxygenases have been developed, our collective results provide what are, to our knowledge, the first development and mechanistic study of a cell-active inhibitor of human RNA demethylase FTO. We utilize structure-guided *in silico* screening and biochemical evaluations in order to discover several potential small-molecule inhibitors of FTO demethylase *in vitro*. The mechanistic study and kinetics analysis of inhibition reveals that the best inhibitor, rhein, can reversibly bind FTO enzyme and competitively prevent the recognition of m^6A substrates. Moreover, rhein also exhibits low cytotoxicity and is capable of increasing the modification level of m^6A in mRNA inside cells, which is likely a result of the ability of rhein to inhibit the demethylation of m^6A by FTO as well as perhaps other cellular demethylases yet to be identified. Nevertheless, this work provides the first identified example of a competitive inhibitor for FTO *in vitro* and inside cells, which can likely be used as a tool compound in coming studies to probe how the cellular status of m^6A in mRNA might affect physiological processes. The workings of the cellular mechanism cannot yet be definitively linked to obesity treatment, which remains an open line of research study. Lastly, the molecular modeling of FTO/rhein complex suggests that this inhibitor has a smaller and more compact chemical structure to gain potency and selectivity through favorable interactions at the active site after further optimization.

The scope and mechanisms of the dynamic mRNA demethylation represent a new frontier in RNA epigenetic research in both aspects of target identification and chemical regulation.[13] FTO was reported to be widely expressed in both fetal and adult tissues, with the highest expression level in brain.[4] The distribution of cellular m^6A modification in mRNA has been recently demonstrated to be widespread throughout the transcriptome.[23,24] The identification of FTO as the m^6A demethylase in RNA has opened new avenues for biological regulation. Certainly, FTO might not be the sole enzyme to regulate the cellular level of m^6A in various mammalian tissues. The functions of several other AlkB human analogues, such as ALKBH4−7, remain largely unknown. We still can speculate that more demethylases exist inside cells, which may be capable of m^6A demodification in addition to FTO. On the other hand, we present the first example that a small molecule can modulate cellular levels of m^6A modification in mRNA. Analogous to the development of the selective inhibitor of Jumonji C domain-containing histone demethylase,[42] selective and specific small-molecule inhibitors for mRNA demethylases, FTO for example, will be achieved by further optimizations, and thus serve as potential leads for new therapies and powerful probes for a wide range of biological pathways. Taken together, the discovery of other nucleic acid demethylases as well as the development of selective regulators will likely enable more studies in the new frontier for RNA demodification biology.

EXPERIMENTAL SECTION

Virtual Screening for Compound Binding at the FTO Active Site. The drug-like SPECS database containing ~100 000 compounds was selected for virtual screening against the known FTO structure (PDB code 3LFM) in Dock4.0. Residues around m^3T within a radius of 6 Å were isolated in order to construct the grid for docking simulation, and the results were analyzed using CScore from Sybyl software package. The compounds with the consensus score of 5 were then rescored in AutoDock4.0. According to predicted binding free energy and geometrical matching quality, the top 300 compounds were selected and classified by scaffold diversity in Pipeline Pilot 5.0. Lastly, 114 compounds were purchased for experimental evaluation. The inhibitory active molecules were used to run a similarity search through an in-house database of older drug therapies using SciTegic functional class fingerprints (FCFP_4) in Pipeline Pilot 5.0.

Inhibition of m^6A Demethylation in ssDNA. The known procedures were followed to express and purify FTO protein,[20] and evaluate the repair of ssDNA containing m^6A in a *Dpn*II cleavage sequence (5′-TAGACATTGCCATTCTCGATAGG(m^6A)-TCCGGTCAAACCTAGACGAATTCCA-3′).[29] The reactions were carried out in 100 μL of buffer (50 mM Tris-HCl, pH 7.5) containing 0.1 nmol of ssDNA, 0.1 nmol of FTO, 300 μM 2OG, 280 μM $(NH_4)_2Fe(SO_4)_2$, 2 mM L-ascorbic acid, and compounds at varying concentrations. After incubation at room temperature for 2 h, the reactions were quenched by heating for 5 min at 90 °C. The ssDNA was annealed to the complementary strand for *Dpn*II digestion. The digestion sample was checked on 20% non-reducing PAGE, and the inhibition percentage was estimated by measuring the intensity of the bands after GelRed staining.

Inhibition of m^6A Demethylation in ssRNA. Based on the published protocol,[12] reactions were typically run on the same scale described for the inhibition of ssDNA demethylation, except for using 15-mer ssRNA (5′-CUUGUCA(m^6A)CAGCAGA-3′) at 10 μM and

dx.doi.org/10.1021/ja3064149 | J. Am. Chem. Soc. 2012, 134, 17963−17971

FTO protein at 1 μM. After incubation at 25 °C for 1 h, the reaction was quenched, and ssRNA was digested by nuclease P1 and alkaline phosphatase. The nucleosides were analyzed on an HPLC system equipped with an Agilent Eclipse XDB-C18 analyses column (150 × 4.6 mm) setting mobile phase of buffer A (25 mM NaH_2PO_4) and buffer B (acetonitrile) at a flow rate of 1 mL/min at room temperature. The detection wavelength was set at 266 nm. IC_{50} value for FTO repair inhibition by rhein was also calculated by using this assay in triplicate.

Isothermal Titration Calorimetry (ITC). ITC experiments were performed at 25 °C using a Microcal iTC_{200} isothermal titration calorimeter (GE Healthcare). Freshly purified FTO protein in a buffer containing 50 mM sodium phosphate (pH 8.0), 300 mM NaCl, and 10 mM β-mercaptoethanol was subjected to ITC experiment. The 0.2 mL sample cell was filled with 40 μM FTO and stirred constantly at 1000 rpm. The syringe was filled with 600 μM rhein and titrated into the sample cell in one 0.4 μL injection, followed by 1.6 μL injections at 600 s intervals. After the background dilution heats were subtracted from the experimental data, the net titration data were analyzed with the Microcal ORIGIN V7.0 software (Microcal Software, Northampton, MA).

Surface Plasmon Resonance (SPR). SPR technology-based binding assays were performed on Biacore 3000 instrument (GE Healthcare) at room temperature. FTO protein was covalently immobilized on CM5 chip by a standard amine-coupling procedure in 10 mM sodium acetate (pH 4.2). The chip was equilibrated with HBS-EP buffer (10 mM HEPES (pH 7.4), 150 mM NaCl, 3 mM EDTA, 0.005% (v/v) surfactant P20) for 2 h. Compounds were serially diluted and injected for 60 s (contact phase) at a flow rate of 20 μL/min, followed by 120 s of buffer flow (dissociation phase). The K_d values of tested compounds were determined by BIA evaluation software (GE Healthcare).

Differential Scanning Fluorimetry (DSF). DSF experiments were performed on a RT-PCR detection system (ABI 7500 Fast) according to the known protocol.[43] SYPRO orange (Invitrogen) was monitored using the filters of FAM at the wavelength of 492 nm for excitation and of ROX at the wavelength of 610 nm for emission. Each reaction solution containing 1.25 μM protein, 5 × SYPRO orange, and tested compound in 30 μL was heated from 25 to 95 °C at 1% ramp rate. Fluorescence intensities were recorded every 0.4 °C and plotted as a function of temperature. The inflection point of the transition curve (T_m) was calculated by fitting the Boltzmann equation to the sigmoidal curve in Origin 8.0. Each condition was tested in triplicate.

Circular Dichroism (CD) Experiment. The CD spectra were recorded on a Jasco J-810 spectropolarimeter at 25 °C. All measurements were taken in a 0.1 cm path length quartz cuvette at the wavelength range of 200−250 nm. The FTO protein (5 μM in 20 mM sodium phosphate, pH 8.0) was treated with varying concentrations of rhein and incubated for 1 h at 25 °C prior to CD analyses. Three consecutive scans were averaged as the reported spectra.

Fluorescence Polarization (FP) Assay. Fluorescein-labeled ssDNA substrate (5′-ATTGTCA (m^6A) CAGCAGA-FAM-3′) was synthesized on an Expedite DNA synthesizer (PerSeptive Biosystems). Serial dilutions of competitors for FTO were prepared from 20 mM DMSO stocks. The diluted compound was added to the reaction mixture in 100 μL of borate buffer (50 mM, pH 7.5) to final concentrations of 25 μM FTO and 50 nM ssDNA. After a 30-min incubation at 25 °C, FP was measured on an EnVision Multilabel Plate Reader using the wavelengths of 480 nm for excitation and 520 nm for emission, respectively. Each reaction was repeated for three times. Binding parameters were calculated from nonlinear regression using GraphPad Prism 5.0.

Kinetics of FTO Inhibition by Rhein. To determine the kinetics value for the inhibition of repair reaction by rhein, initial rates were obtained by keeping a constant FTO concentration of 0.05 μM and varying the substrate ssRNA concentration ranging from 0.5 to 2.0 μM in the presence of inhibitor rhein at a concentration of 0, 2.0, and 4.0 μM, respectively. Reactions were adjusted to ensure that less than 20% of the substrate was consumed, and quenched by heating for 5 min at 90 °C. After treatment of nuclease P1 and alkaline phosphatase, the nucleosides were separated by reverse-phase ultra-performance liquid chromatography setting mobile phase of buffer A (water containing 1‰ Formic acid) and buffer B (acetonitrile) in a flow rate of 0.3 mL/min, coupled with online Agilent 6460 Triple Quad LC/MS detection, and quantified using the nucleoside to base ion mass transitions of 282 to 150 (m^6A), 268 to 136 (A), and 284 to 152 (G). The K_m and K_i values were determined with the Michaelis−Menten equation fits and Lineweaver−Burk plot in GraphPad Prism 5.0.

Inhibition of m^6A Demethylation in Cells. Knockdown of FTO in BE(2)-C cell line by transient transfection of siRNA was performed according to the published procedure.[12] Tested compounds were freshly dissolved into cell media before feeding to cells at concentrations of 10−50 μM. After a 24-h incubation, cells were harvested and the total cellular mRNA was isolated and digested by nuclease P1 and alkaline phosphatase following standard protocol. The nucleosides were separated by reverse phase ultraperformance liquid chromatography coupled with online triple-quadrupole LC mass spectrometer detection, and quantified by comparison with the standard curve obtained from pure nucleoside standards running at the same batch of samples. The ratio of m^6A to A was calculated on the basis of the calculated concentrations.

Molecular Modeling. According to molecular docking results, four structural models of rhein/FTO complex with different orientation of carboxyl in rhein were selected for molecular dynamic simulations in a time scale of 10 ns using Gromacs 4.5.3. On the basis of the equilibrated dynamic trajectories, a total of 200 snapshots were extracted from the last 1-ns trajectory in order to calculate the free binding energy of the four rhein/FTO complexes by using the MM-GBSA method encoded in the AMBER 10 program.[44] The binding energy of the residues in the active site pocket was decomposed in order to investigate the partial energy contributions of each residue upon substrate binding.

■ ASSOCIATED CONTENT

Supporting Information

Additional experimental methods and Figures S1−S10 and Tables S1 and S2 as mentioned in text. This material is available free of charge via the Internet at http://pubs.acs.org.

■ AUTHOR INFORMATION

Corresponding Author

cluo@mail.shcnc.ac.cn; yangcg@mail.shcnc.ac.cn

Author Contributions

⊥B.C., F.Y., and L.Y. contributed equally.

Notes

The authors declare no competing financial interest.

■ ACKNOWLEDGMENTS

We thank C. Li for help with SPR assay, and S. F. Reichard, MA, for editing the manuscript. This work was supported by the Chinese Academy of Sciences (the Hundred Talent Program to C.-G.Y. and XDA01040305 to C.L.), the National Natural Science Foundation of China (20972173, 90913010, 20972174, 21021063, 91029704, and 21210003), the Hi-Tech Research and Development Program of China (2012AA020302), the State Key Program of Basic Research of China Grant (2009CB918502). Computation resources were partially supported by Computer Network Information Center, Chinese Academy of Sciences and Shanghai Supercomputing Center.

■ REFERENCES

(1) Dina, C.; Meyre, D.; Gallina, S.; Durand, E.; Korner, A.; Jacobson, P.; Carlsson, L. M.; Kiess, W.; Vatin, V.; Lecoeur, C.; Delplanque, J.; Vaillant, E.; Pattou, F.; Ruiz, J.; Weill, J.; Levy-Marchal,

C.; Horber, F.; Potoczna, N.; Hercberg, S.; Le Stunff, C.; Bougneres, P.; Kovacs, P.; Marre, M.; Balkau, B.; Cauchi, S.; Chevre, J. C.; Froguel, P. *Nat. Genet.* **2007**, *39*, 724.
(2) Thorleifsson, G.; Holm, H.; Edvardsson, V.; Walters, G. B.; Styrkarsdottir, U.; Gudbjartsson, D. F.; Sulem, P.; Halldorsson, B. V.; de Vegt, F.; d'Ancona, F. C.; den Heijer, M.; Franzson, L.; Christiansen, C.; Alexandersen, P.; Rafnar, T.; Kristjansson, K.; Sigurdsson, G.; Kiemeney, L. A.; Bodvarsson, M.; Indridason, O. S.; Palsson, R.; Kong, A.; Thorsteinsdottir, U.; Stefansson, K. *Nat. Genet.* **2009**, *41*, 926.
(3) Scott, L. J.; Mohlke, K. L.; Bonnycastle, L. L.; Willer, C. J.; Li, Y.; Duren, W. L.; Erdos, M. R.; Stringham, H. M.; Chines, P. S.; Jackson, A. U.; Prokunina-Olsson, L.; Ding, C. J.; Swift, A. J.; Narisu, N.; Hu, T.; Pruim, R.; Xiao, R.; Li, X. Y.; Conneely, K. N.; Riebow, N. L.; Sprau, A. G.; Tong, M.; White, P. P.; Hetrick, K. N.; Barnhart, M. W.; Bark, C. W.; Goldstein, J. L.; Watkins, L.; Xiang, F.; Saramies, J.; Buchanan, T. A.; Watanabe, R. M.; Valle, T. T.; Kinnunen, L.; Abecasis, G. R.; Pugh, E. W.; Doheny, K. F.; Bergman, R. N.; Tuomilehto, J.; Collins, F. S.; Boehnke, M. *Science* **2007**, *316*, 1341.
(4) Frayling, T. M.; Timpson, N. J.; Weedon, M. N.; Zeggini, E.; Freathy, R. M.; Lindgren, C. M.; Perry, J. R.; Elliott, K. S.; Lango, H.; Rayner, N. W.; Shields, B.; Harries, L. W.; Barrett, J. C.; Ellard, S.; Groves, C. J.; Knight, B.; Patch, A. M.; Ness, A. R.; Ebrahim, S.; Lawlor, D. A.; Ring, S. M.; Ben-Shlomo, Y.; Jarvelin, M. R.; Sovio, U.; Bennett, A. J.; Melzer, D.; Ferrucci, L.; Loos, R. J.; Barroso, I.; Wareham, N. J.; Karpe, F.; Owen, K. R.; Cardon, L. R.; Walker, M.; Hitman, G. A.; Palmer, C. N.; Doney, A. S.; Morris, A. D.; Smith, G. D.; Hattersley, A. T.; McCarthy, M. I. *Science* **2007**, *316*, 889.
(5) Fischer, J.; Koch, L.; Emmerling, C.; Vierkotten, J.; Peters, T.; Bruning, J. C.; Ruther, U. *Nature* **2009**, *458*, 894.
(6) Church, C.; Moir, L.; McMurray, F.; Girard, C.; Banks, G. T.; Teboul, L.; Wells, S.; Bruning, J. C.; Nolan, P. M.; Ashcroft, F. M.; Cox, R. D. *Nat. Genet.* **2010**, *42*, 1086.
(7) Pausova, Z.; Syme, C.; Abrahamowicz, M.; Xiao, Y.; Leonard, G. T.; Perron, M.; Richer, L.; Veillette, S.; Smith, G. D.; Seda, O.; Tremblay, J.; Hamet, P.; Gaudet, D.; Paus, T. *Circ. Cardiovasc. Genet.* **2009**, *2*, 260.
(8) Hotta, K.; Kitamoto, T.; Kitamoto, A.; Mizusawa, S.; Matsuo, T.; Nakata, Y.; Kamohara, S.; Miyatake, N.; Kotani, K.; Komatsu, R.; Itoh, N.; Mineo, I.; Wada, J.; Yoneda, M.; Nakajima, A.; Funahashi, T.; Miyazaki, S.; Tokunaga, K.; Masuzaki, H.; Ueno, T.; Hamaguchi, K.; Tanaka, K.; Yamada, K.; Hanafusa, T.; Oikawa, S.; Yoshimatsu, H.; Sakata, T.; Matsuzawa, Y.; Nakao, K.; Sekine, A. *J. Hum. Genet.* **2011**, *56*, 647.
(9) Wehr, E.; Schweighofer, N.; Moller, R.; Giuliani, A.; Pieber, T. R.; Obermayer-Pietsch, B. *Metabolism* **2010**, *59*, 575.
(10) Keller, L.; Xu, W.; Wang, H. X.; Winblad, B.; Fratiglioni, L.; Graff, C. *J. Alzheimers Dis.* **2011**, *23*, 461.
(11) Kaklamani, V.; Yi, N.; Sadim, M.; Siziopikou, K.; Zhang, K.; Xu, Y.; Tofilon, S.; Agarwal, S.; Pasche, B.; Mantzoros, C. *BMC Med .Genet* **2011**, *12*, 52.
(12) Jia, G.; Fu, Y.; Zhao, X.; Dai, Q.; Zheng, G.; Yang, Y.; Yi, C.; Lindahl, T.; Pan, T.; Yang, Y. G.; He, C. *Nat. Chem. Biol.* **2011**, *7*, 885.
(13) He, C. *Nat. Chem. Biol.* **2010**, *6*, 863.
(14) Gerken, T.; Girard, C. A.; Tung, Y. C.; Webby, C. J.; Saudek, V.; Hewitson, K. S.; Yeo, G. S.; McDonough, M. A.; Cunliffe, S.; McNeill, L. A.; Galvanovskis, J.; Rorsman, P.; Robins, P.; Prieur, X.; Coll, A. P.; Ma, M.; Jovanovic, Z.; Farooqi, I. S.; Sedgwick, B.; Barroso, I.; Lindahl, T.; Ponting, C. P.; Ashcroft, F. M.; O'Rahilly, S.; Schofield, C. J. *Science* **2007**, *318*, 1469.
(15) Kurowski, M. A.; Bhagwat, A. S.; Papaj, G.; Bujnicki, J. M. *BMC Genomics* **2003**, *4*, 48.
(16) Trewick, S. C.; Henshaw, T. F.; Hausinger, R. P.; Lindahl, T.; Sedgwick, B. *Nature* **2002**, *419*, 174.
(17) Falnes, P. O.; Johansen, R. F.; Seeberg, E. *Nature* **2002**, *419*, 178.
(18) Fu, Y.; Dai, Q.; Zhang, W.; Ren, J.; Pan, T.; He, C. *Angew. Chem., Int. Ed.* **2010**, *49*, 8885.
(19) van den Born, E.; Vagbo, C. B.; Songe-Moller, L.; Leihne, V.; Lien, G. F.; Leszczynska, G.; Malkiewicz, A.; Krokan, H. E.; Kirpekar, F.; Klungland, A.; Falnes, P. O. *Nat. Commun.* **2011**, *2*, 172.
(20) Jia, G.; Yang, C. G.; Yang, S.; Jian, X.; Yi, C.; Zhou, Z.; He, C. *FEBS Lett.* **2008**, *582*, 3313.
(21) Lee, D. H.; Jin, S. G.; Cai, S.; Chen, Y.; Pfeifer, G. P.; O'Connor, T. R. *J. Biol. Chem.* **2005**, *280*, 39448.
(22) Desrosiers, R.; Friderici, K.; Rottman, F. *Proc. Natl. Acad. Sci. U.S.A.* **1974**, *71*, 3971.
(23) Dominissini, D.; Moshitch-Moshkovitz, S.; Schwartz, S.; Salmon-Divon, M.; Ungar, L.; Osenberg, S.; Cesarkas, K.; Jacob-Hirsch, J.; Amariglio, N.; Kupiec, M.; Sorek, R.; Rechavi, G. *Nature* **2012**, *485*, 201.
(24) Meyer, K. D.; Saletore, Y.; Zumbo, P.; Elemento, O.; Mason, C. E.; Jaffrey, S. R. *Cell* **2012**, *149*, 1635.
(25) Tung, Y. C.; Yeo, G. S. *Ann. N.Y. Acad. Sci.* **2011**, *1220*, 162.
(26) Han, Z.; Niu, T.; Chang, J.; Lei, X.; Zhao, M.; Wang, Q.; Cheng, W.; Wang, J.; Feng, Y.; Chai, J. *Nature* **2010**, *464*, 1205.
(27) Yi, C.; Yang, C. G.; He, C. *Acc. Chem. Res.* **2009**, *42*, 519.
(28) Yu, B.; Edstrom, W. C.; Benach, J.; Hamuro, Y.; Weber, P. C.; Gibney, B. R.; Hunt, J. F. *Nature* **2006**, *439*, 879.
(29) Yang, C. G.; Yi, C.; Duguid, E. M.; Sullivan, C. T.; Jian, X.; Rice, P. A.; He, C. *Nature* **2008**, *452*, 961.
(30) Sundheim, O.; Vagbo, C. B.; Bjoras, M.; Sousa, M. M.; Talstad, V.; Aas, P. A.; Drablos, F.; Krokan, H. E.; Tainer, J. A.; Slupphaug, G. *Embo J.* **2006**, *25*, 3389.
(31) Yi, C.; Jia, G.; Hou, G.; Dai, Q.; Zhang, W.; Zheng, G.; Jian, X.; Yang, C. G.; Cui, Q.; He, C. *Nature* **2010**, *468*, 330.
(32) Rose, N. R.; McDonough, M. A.; King, O. N.; Kawamura, A.; Schofield, C. J. *Chem. Soc. Rev.* **2011**, *40*, 4364.
(33) Chang, P. C.; Wang, J. D.; Lee, M. M.; Chang, S. S.; Tsai, T. Y.; Chang, K. W.; Tsai, F. J.; Chen, C. Y. *J. Biomol. Struct. Dyn.* **2011**, *29*, 471.
(34) Crain, P. F. *Methods Enzymol.* **1990**, *193*, 782.
(35) Woon, E. C.; Demetriades, M.; Bagg, E. A.; Aik, W.; Krylova, S. M.; Ma, J. H.; Chan, M.; Walport, L. J.; Wegman, D. W.; Dack, K. N.; McDonough, M. A.; Krylov, S. N.; Schofield, C. J. *J. Med. Chem.* **2012**, *55*, 2173.
(36) Welford, R. W.; Schlemminger, I.; McNeill, L. A.; Hewitson, K. S.; Schofield, C. J. *J. Biol. Chem.* **2003**, *278*, 10157.
(37) Jia, Z. H.; Liu, Z. H.; Zheng, J. M.; Zeng, C. H.; Li, L. S. *Exp. Clin. Endocrinol. Diabetes* **2007**, *115*, 571.
(38) He, Z. H.; He, M. F.; Ma, S. C.; But, P. P. *J. Ethnopharmacol.* **2009**, *121*, 313.
(39) Gao, Q.; Qin, W. S.; Jia, Z. H.; Zheng, J. M.; Zeng, C. H.; Li, L. S.; Liu, Z. H. *Planta Med.* **2010**, *76*, 27.
(40) Zhang, H.; Chen, L.; Chen, J.; Jiang, H.; Shen, X. *J. Biol. Chem.* **2011**, *286*, 24593.
(41) http://pubchem.ncbi.nlm.nih.gov/summary/summary.cgi?cid=10168&loc=ec_rcs.
(42) Luo, X.; Liu, Y.; Kubicek, S.; Myllyharju, J.; Tumber, A.; Ng, S.; Che, K. H.; Podoll, J.; Heightman, T. D.; Oppermann, U.; Schreiber, S. L.; Wang, X. *J. Am. Chem. Soc.* **2011**, *133*, 9451.
(43) Niesen, F. H.; Berglund, H.; Vedadi, M. *Nat. Protoc.* **2007**, *2*, 2212.
(44) Kollman, P. A.; Massova, I.; Reyes, C.; Kuhn, B.; Huo, S.; Chong, L.; Lee, M.; Lee, T.; Duan, Y.; Wang, W.; Donini, O.; Cieplak, P.; Srinivasan, J.; Case, D. A.; Cheatham, T. E., III *Acc. Chem. Res.* **2000**, *33*, 889.